J Mater Sci: Mater Med (2011) 22:2231–2237
DOI 10.1007/s10856-011-4410-8

Deposition of TiN films on Co–Cr for improving mechanical properties and biocompatibility using reactive DC sputtering

Vuong-Hung Pham · Se-Won Yook · Eun-Jung Lee · Yuanlong Li · Gyuran Jeon · Jung-Joong Lee · Hyoun-Ee Kim · Young-Hag Koh

Received: 4 March 2011 / Accepted: 28 July 2011 / Published online: 13 August 2011

Abstract This study reports the deposition of TiN films on Co–Cr substrates to improve the substrates' mechanical properties and biological properties. In particular, the argon to nitrogen ($Ar:N_2$) gas flow ratio was adjusted to control the microstructure of the TiN films. A Ti interlayer was also used to enhance the adhesion strength between the Co–Cr substrate and TiN films. A series of TiN films, which are denoted as TiN-(Ar/N_2)1:1, Ti/TiN-(Ar/N_2)1:1, and Ti/TiN-($Ar:N_2$)1:3, were deposited by reactive DC sputtering. All the deposited TiN films showed a dense, columnar structure with a preferential orientation of the (200) plane. These TiN films increased the mechanical properties of Co–Cr, such as the critical load during scratch testing, hardness, elastic modulus and plastic resistance. In addition, the biological properties of the Co–Cr substrates, i.e. initial attachment, proliferation, and cellular differentiation of the MC3T3-E1 cells, were improved considerably by deposition of the TiN films. These results suggest that TiN films would effectively enhance both the mechanical properties and biocompatibility of biomedical Co–Cr alloys.

V.-H. Pham · S.-W. Yook · E.-J. Lee · Y. Li · G. Jeon · J.-J. Lee · H.-E. Kim (✉)
WCU Hybrid Materials Program, Department of Materials Science and Engineering, Seoul National University, Seoul 151-744, Korea
e-mail: kimhe@snu.ac.kr

Y.-H. Koh
Department of Dental Laboratory Science and Engineering, Korea University, Seoul 136-703, Korea

1 Introduction

Co–Cr alloys are recognized as one of the most suitable materials for biomedical applications, such as load-bearing joint replacements (hip or knee), dental implants and stents, on account of their outstanding chemical stability, mechanical properties and biocompatibility [1–3]. Fundamentally, the biocompatibility of Co–Cr alloys can be attributed to the surface oxide layer, which is formed naturally in air [4]. However, these materials have relatively low surface hardness and wear resistance [5, 6], which has caused concern about the potential release of metal ions after implantation [7–9].

Surface modification is used widely to improve the biocompatibility of metallic implants, because it can tailor the surface characteristics to be favorable for the growth, proliferation and differentiation of osteoblasts in an easy and economical manner [10–12]. One of the most promising surface modification techniques is to coat the surface of metallic implants with biocompatible materials, including microporous TiO_2 [13] and TiN films [14]. In particular, TiN films have been proven to be the effective materials for improving the mechanical properties of relatively soft metals and alloys, such as hardness, wear resistance, and corrosion resistance [15–17]. In addition, TiN films can enhance the biocompatibility of biomedical metals significantly [18, 19] because of TiN's biocompatibility [20, 21]. More recently, it was reported that TiN films with a controlled microstructure could be deposited successfully on Co–Cr substrates by applying a negative substrate bias during reactive DC sputtering, which could lead to a significant increase in surface hardness [22]. However, little attention has been directed towards the evaluation of the cell attachment, proliferation and differentiation of osteoblasts cells on TiN-coated Co–Cr alloys.

Therefore, in this study, TiN films were deposited on Co–Cr substrates by reactive DC sputtering. The Ar:N_2 gas flow ratio was adjusted to control the microstructure of the TiN films. A series of TiN films were deposited on Co–Cr substrates, which are denoted as TiN-(Ar/N_2)1:1, Ti/TiN-(Ar/N_2)1:1, and Ti/TiN-(Ar:N_2)1:3. The microstructure and crystal structure of the TiN coatings were characterized by field emission scanning electron microscopy (FE-SEM) and X-ray diffraction (XRD), respectively. The mechanical properties of the TiN films deposited Co–Cr substrates were evaluated by scratch testing and ultra-low load microhardness testing, respectively. Pre-osteoblast cells (MC3T3-E1) were used for a biological evaluation in terms of cell attachment, proliferation and differentiation.

2 Materials and methods

2.1 Deposition of TiN films

A series of TiN films were deposited onto Co–Cr substrates by DC sputtering (Ultech, Daegu, Korea), where a Ar:N_2 gas flow ratio, which is one of the most important processing parameters was adjusted to control the microstructure of the TiN films. Prior to deposition, the Co–Cr substrates (Bukang Coalloy, Korea) with dimensions of 10 mm × 10 mm × 1 mm or 25 mm × 25 mm × 1 mm were ground with a 2000-grit SiC abrasive paper and cleaned ultrasonically. The deposition chamber was pumped to 5×10^{-4} Pa using rotary and diffusion pumps. The substrate was then subjected to ion bombardment in an argon flow discharge under a negative bias voltage of 600 V for 30 min to remove any residual surface contamination. Subsequently, the Ti and TiN films were deposited by reactive DC sputtering of a Ti target (diameter 75 mm, thickness 5 mm, purity 99.9%, Kahee Metal, Korea). Pre-sputtering of a thin titanium layer at a substrate temperature of 400°C was performed for 15 min. This layer would be expected to act as an interlayer to enhance the adhesion between the substrate and TiN films [23]. Subsequently, high purity argon (99.998% pure) and nitrogen (99.9995% pure) gases were introduced at various flow ratios (1:1 and 1:3) for the deposition of TiN films, denoted as Ti/TiN-(Ar:N_2)1:1 and Ti/TiN-(Ar:N_2)1:3 films, respectively. For comparison, a TiN film was deposited at an Ar:N_2 flow ratio of 1:1 without a Ti interlayer (TiN-(Ar:N_2)1:1 film). The substrate temperature was 400°C and the current was kept constant at 0.6 A for the deposition of all the TiN films.

2.2 Structural characterization

The crystalline of the TiN films deposited on Co–Cr substrates were examined by X-ray diffraction (XRD; M18XHF-SRA, Mac Science Co, Yokohama, Japan) using CuK_α radiation. The scan rate used was 1°/min and the scan range was from 30° to 80°. The microstructure and surface morphology of TiN films deposited on Co–Cr substrates were studied by field emission scanning electron microscopy (FE-SEM; JEOL, JSM-6330F, JEOL Techniques, Tokyo, Japan) operated at 15 kV.

2.3 Mechanical properties

The adhesion strength was measured using a scratch tester (CSEM Instruments, Revetest, Scratch-tester, Switzerland) by employing the acoustic emission (AE) fluctuations and optical microscopy. The coated surface was scratched with a conical Rockwell C tip with a radius of 200 μm. Scratches (5 mm in length) were made with a linear speed of 5 mm/min, where the applied loads ranged from 0 to 30 N. It is essential to define two different critical loads in order to give an accurate description of adhesion failure [24]. According to Gerth, the first critical load, L_1, is the load at which the first sporadic isolated adhesion failure takes place. The second critical load, L_2, is the load at which more continuously spread adhesion failure begins. Two identical scratches were made in each sample. In this study, AE signal intensity was continuously monitored and failure modes L_1 and L_2 were clearly identified with the increase in the AE signal during scratching. The results were verified by optical microscope at 40× magnification to determine the value of the critical load.

Microhardness tests were performed to measure the mechanical properties of the TiN films. The microhardness (H) and elastic modulus (E) were calculated from the load/upload curves obtained using a computer controlled microhardness tester. Ultra low microindentation (Fischerscope H100, Germany) was performed under a Vicker's diamond indenter load, L = 15 mN. The total penetration of the indenter into the film was set to 10% of the films' thickness. Each datum was an average of ten indentations. The load-indentation depth profiles were recorded automatically during indentation.

2.4 Biological properties

Pre-osteoblasts MC3T3-E1 (ATCC, CRL-2593) were used to examine the interaction between the cell and specimens (uncoated Co–Cr substrate, Ti/TiN-(Ar:N_2)1:1 film, Ti/TiN-(Ar:N_2)1:3 film). The cells were maintained in α-MEM containing 10% fetal bovine serum (FBS) and 1% antibiotic at 37°C in humidified air and 5% CO_2. The cell attachment was visualized by confocal laser scanning microscopy (CLMS, Zeiss-LSM510, Carl Zeiss Inc., NY, USA). After culturing for 24 h, the cells on the tested sample were fixed in 4% paraformaldehyde in PBS for

10 min, washed in PBS, permeabilized with 0.1% Triton X-100 in PBS in 7 min, washed in PBS and stained with fluorescent phalloidin for 30 min. The cell nuclei were counterstained with DAPI for 5 min. The stained samples were placed on a cover slide, and the cell morphology was observed.

The rate of proliferation was measured after culturing for up to 5 days using 3-(4,5-dimethylthiazol-2-yl)-5-(3-carboxy-methoxyphenyl)-2-(-4-sulfophenyl)-2H-tetrazolium (MTS, Promega, Madison, WI, USA) for mitochondrial reduction. The cells (1×10^4 cell/ml) were seeded on the specimens (uncoated Co–Cr substrate, Ti/TiN-(Ar:N_2)1:1 film, Ti/TiN-(Ar:N_2)1:3 film) and cultured for 5 days. They were then washed with PBS and placed in a culture medium containing the MTS solution and returned to the incubator at 37°C for 3 h. This assay is based on the ability of metabolically active cells to reduce a tetrazolium-based compound, MTS, to a purple formazan product. The quantity of formazan product, which is measured by the absorbance at 490 nm using a micro-reader (Biorad, Model 550, USA), is directly proportional to the number of living cells in the culture.

The extent of cell differentiation was assessed by measuring the alkaline phosphatase (ALP) activity of the cells cultured on the specimens (uncoated Co–Cr substrate, Ti/TiN-(Ar:N_2)1:1 film, Ti/TiN-(Ar:N_2)1:3 film). The cells (1×10^4 cell/ml) were seeded on the specimens and cultured for 7 days. They were then washed with PBS and detached using trypsin-ethylene diamine tetraacetic acid. The amount of protein in the cell lysates was quantified using a protein assay kit (Biorad, Hercules, CA, USA) and the ALP activity was assayed calorimetrically using *p*-nitrophenyl phosphate (pNPP, Sigma-Aldrich, UK). This colorimetric assay is based on the conversion of pNPP to *p*-nitrophenol (pNP) in the presence of ALP, where the rate of pNP production is proportional to the ALP activity. The absorbance of the reaction product, pNP, was measured at 405 nm using a microplate reader.

The data is presented as the mean ± standard deviation. Statistical analysis was performed using a *t* test. A *P* value <0.05 was considered significant.

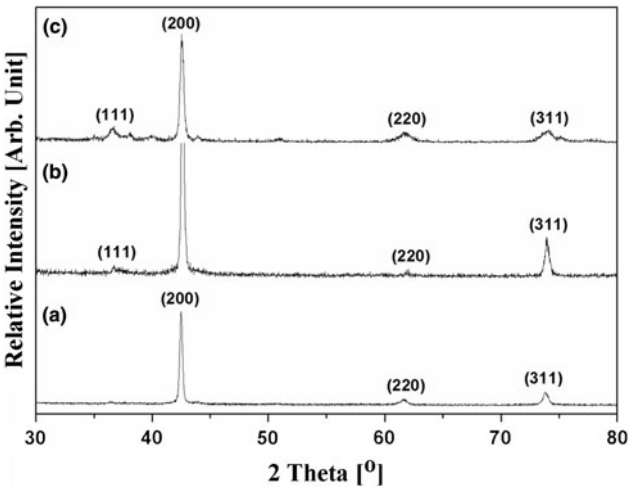

Fig. 1 XRD patterns of (*a*) TiN-(Ar:N_2)1:1 film, (*b*) Ti/TiN-(Ar:N_2)1:1 film, and (*c*) Ti/TiN-(Ar:N_2)1:3 film

3 Results and discussion

3.1 Structural characterization of TiN films

Figure 1a–c shows typical XRD patterns of the TiN-(Ar:N_2)1:1, Ti/TiN-(Ar:N_2)1:1, and Ti/TiN-(Ar:N_2)1:3 films deposited Co–Cr substrates. Without a Ti interlayer, the TiN film showed three crystalline peaks corresponding to the (200), (220), and (311) planes of the TiN structure (JCPDS card No. 87-0628), as shown in Fig. 1a. On the other hand, when the TiN interlayer was used, an additional peak corresponding to the (111) plane of the crystalline TiN structure was also observed, as shown in Fig. 1b, c. However, all the deposited TiN films were preferentially orientated along the (200) plane. This suggests that the TiN films grew with a columnar structure with a growth direction, (200), parallel to the flux of the incident energetic particles during reactive DC sputtering [25].

Figure 2a–c shows typical cross-sectional SEM images of the TiN-(Ar/N_2)1:1, Ti/TiN-(Ar/N_2)1:1, and Ti/TiN-(Ar:N_2)1:3 films deposited on the Co–Cr substrates. Basically, all the TiN films deposited had a dense columnar structure with an overall thickness of ~2 μm, which was

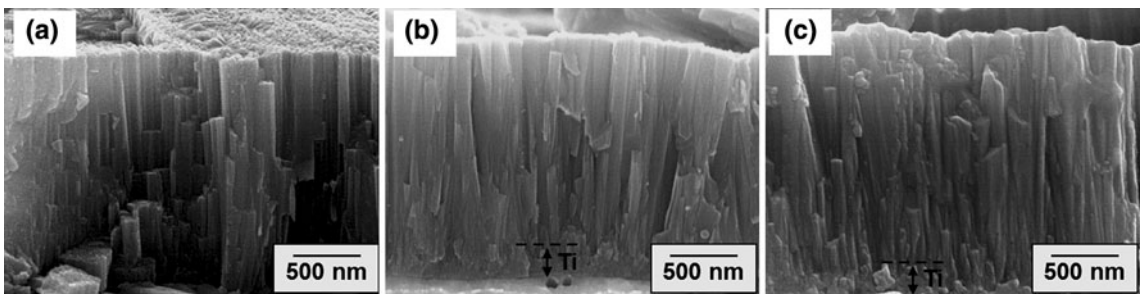

Fig. 2 FE-SEM images showing cross-sections of (**a**) TiN-(Ar:N_2)1:1 film, (**b**) Ti/TiN-(Ar:N_2)1:1 film, and (**c**) Ti/TiN-(Ar:N_2)1:3 film

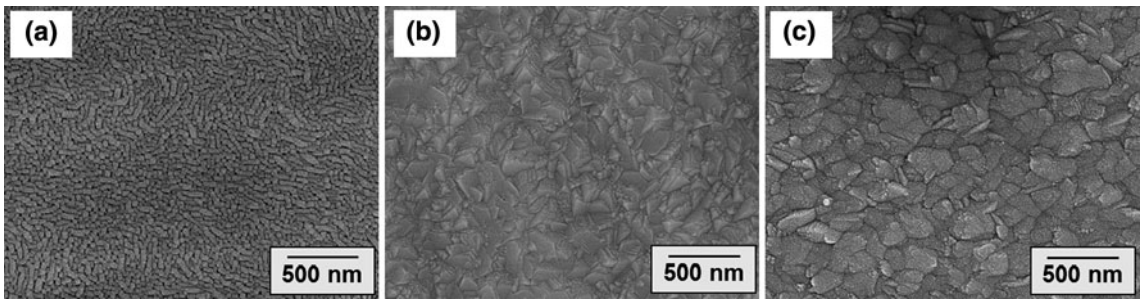

Fig. 3 FE-SEM images showing the surface morphology of (**a**) TiN-(Ar:N_2)1:1 film, (**b**) Ti/TiN-(Ar:N_2)1:1 film, and (**c**) Ti/TiN-(Ar:N_2)1:3 film

corresponded to the XRD results (Fig. 1a–c). In addition, a dense, uniform Ti interlayer with a thickness of ~150 nm was formed for the Ti/TiN-(Ar/N_2)1:1 (Fig. 2b) and Ti/TiN-(Ar:N_2)1:3 films (Fig. 2c), which would be expected to enhance the adhesion between the Co–Cr substrates and TiN films.

Figure 3a–c shows the surface morphology of the TiN-(Ar:N_2)1:1, Ti/TiN-(Ar:N_2)1:1, and Ti/TiN-(Ar:N_2)1:3 films. Although all the TiN films showed a similar columnar microstructure in the cross-sectional view (Fig. 2a–c), they had very different surface morphologies. In other words, the TiN film deposited without a Ti interlayer showed faceted columnar grain morphology (Fig. 3a). On the other hand, a large number of relatively rounded grains were also observed on the Ti/TiN-(Ar:N_2)1:1 film (Fig. 3b). This microstructural change from a faceted to rounded morphology became more widespread for the Ti/TiN-(Ar:N_2)1:3 film (Fig. 3c). In addition, the Ti/TiN-(Ar:N_2)1:3 film showed denser microstructure than the TiN-(Ar/N_2)1:1 and Ti/TiN-(Ar/N_2)1:1 films. This suggests that the microstructure of the TiN films can be controlled by adjusting the Ar:N_2 ratio, which is one of the important processing parameters during reactive sputtering processes [26].

3.2 Mechanical properties

Fundamentally, the lifetime and performance of the coated component may be determined primarily by the adhesion of the coating layer to the substrate [24]. A thin Ti interlayer with a thickness of ~150 nm was used to enhance

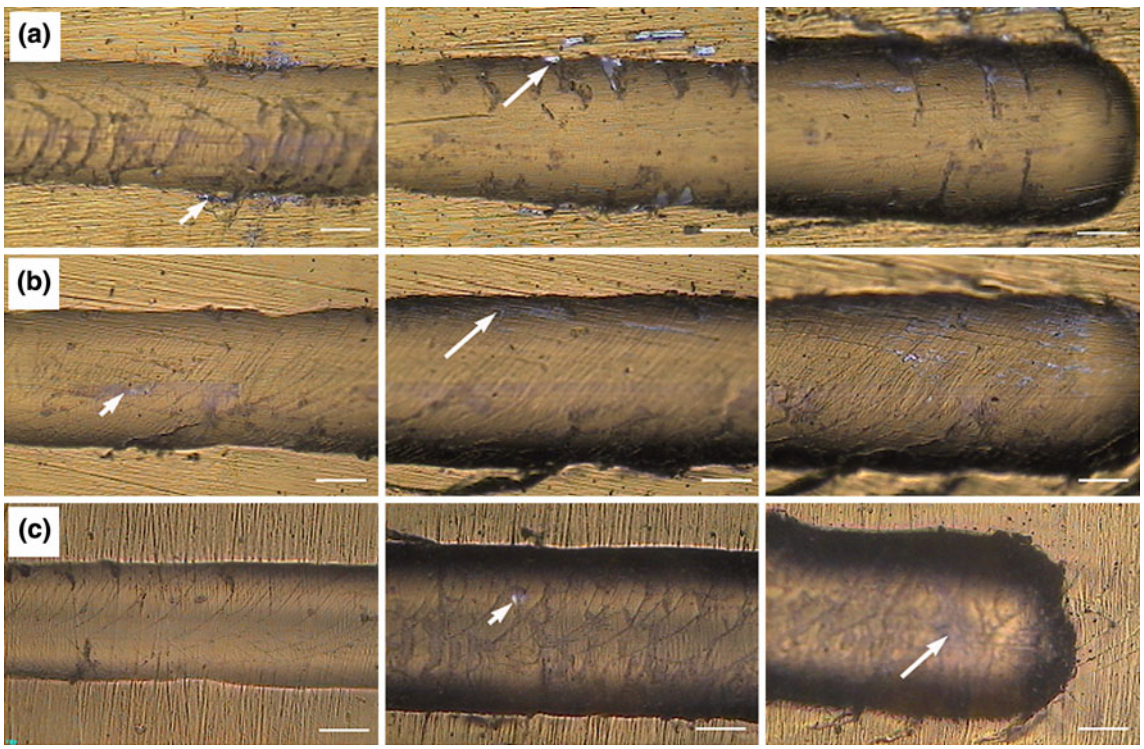

Fig. 4 Optical images of the scratch tested specimens: (**a**) TiN-(Ar:N_2)1:1 film, (**b**) Ti/TiN-(Ar:N_2)1:1 film, and (**c**) Ti/TiN-(Ar:N_2)1:3 film. The scratch direction is from left to right and scale bars indicate 100 μm. The *short arrows* and *long arrows* indicate the critical load L_1 and L_2, respectively

Table 1 Critical load results on the specimens (TiN-(Ar:N_2)1:1, Ti/TiN-(Ar:N_2)1:1, and Ti/TiN-(Ar:N_2)1:3 films)

Critical load	Specimens		
	TiN-(Ar:N_2)1:1 film	Ti/TiN-(Ar:N_2)1:1 film	Ti/TiN-(Ar:N_2)1:3 film
L_1 (N)	10 ± 1	23 ± 4	26 ± 1
L_2 (N)	16 ± 1	25 ± 1	29 ± 2

Table 2 Hardness, elastic modulus and H^3/E^2 results of the specimens (uncoated Co–Cr, TiN-(Ar:N_2)1:1, Ti/TiN-(Ar:N_2)1:1, and Ti/TiN-(Ar:N_2)1:3 films

Specimen	H (GPa)	E (GPa)	H^3/E^2
Co–Cr	4.0 ± 0.3	197 ± 15	0.001 ± 0.0001
TiN-(Ar:N_2)1:1 film	24 ± 3	323 ± 22	0.149 ± 0.05
Ti/TiN-(Ar:N_2)1:1 film	25 ± 3	330 ± 19	0.151 ± 0.09
Ti/TiN-(Ar:N_2)1:3 film	30 ± 4	314 ± 28	0.263 ± 0.08

the adhesion between the TiN film and Co–Cr substrate. This Ti interlayer was calculated from deposition rate (10 nm/min) and the result was verified by cross-sectional SEM images (Fig. 2b, c). Figure 4a–c shows typical optical images of the TiN-(Ar:N_2)1:1, TiN-(Ar:N_2)1:1, and Ti/TiN-(Ar:N_2)1:3 films after the scratch test, where a high critical load was achieved without any obvious cracks on the tested surface. Based on these observations, the critical loads of the TiN films were verified, as summarized in Table 1. The TiN films deposited with the Ti interlayer showed much higher critical loads than that of the TiN film deposited without a Ti interlayer (Table 1), which was attributed mainly to a change in surface morphology (Fig. 3a–c). The Ti/TiN-(Ar:N_2)1:3 film showed the highest critical load owing to its denser microstructure.

Figure 5a–d shows the representative loading-indentation depth curves obtained from microindentation of the uncoated Co–Cr alloy, TiN-(Ar:N_2)1:1, TiN-(Ar:N_2)1:1, and Ti/TiN-(Ar:N_2)1:3 films. Compared to the uncoated Co–Cr, a smaller indentation depth was observed at the same load for all TiN films deposited with or without the Ti interlayer. This suggests that intensive surface hardening was induced successfully by the reactive DC sputtering of TiN films in the Ar:N_2 gas mixture. The average hardness, elastic modulus and the plastic resistance ratio H^3/E^2 of the TiN-(Ar:N_2)1:1, Ti/TiN-(Ar:N_2)1:1, Ti/TiN-(Ar:N_2)1:3 films and uncoated Co–Cr substrate were calculated from the loading-indentation depth curves, as summarized in Table 2. As expected, the deposition of the TiN films increased the hardness and elastic modulus of the Co–Cr significantly (by factors of >6 and >1.6, respectively). In addition, the plastic resistance ratio increased remarkably.

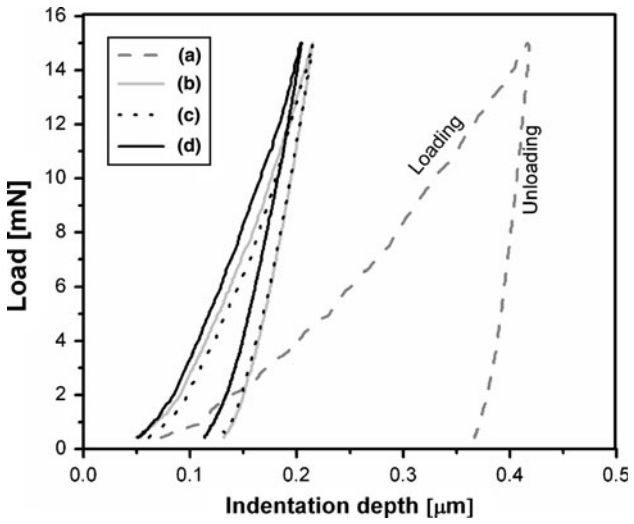

Fig. 5 Typical load-indentation depth curves of the specimens obtained using a microindenter: (*a*) Co–Cr, (*b*) TiN-(Ar:N_2)1:1 film, (*c*) Ti/TiN-(Ar:N_2)1:1 film, and (*d*) Ti/TiN-(Ar:N_2)1:3 film

3.3 Biocompatibility

The biological properties of the Ti/TiN-(Ar:N_2)1:1 and Ti/TiN-(Ar:N_2)1:3 films were evaluated and compared with those of the uncoated Co–Cr substrate. Figure 6a–c shows representative CLMS images of the pre-osteoblast MC3T3-E1 cells grown on an uncoated Co–Cr substrate, Ti/TiN-(Ar:N_2)1:1, and Ti/TiN-(Ar:N_2)1:3 films after culturing for 24 h. All the specimens showed cells that were attached and spread well, suggesting good biocompatibility. However, most of the cells cultured on the Ti/TiN-(Ar:N_2)1:1 and Ti/TiN-(Ar:N_2)1:3 films had a flat morphology and appeared to be adhered intimately to the surface, indicating excellent initial attachment (Fig. 6b, c). In addition, the cellular growth was denser than that on the uncoated Co–Cr substrate.

The change in morphology which is one of the leading indicators of the cell phenotype, will affect the cell-attachment and proliferation kinetics [27]. Figure 7 shows the cell proliferation on the uncoated Co–Cr substrate, Ti/TiN-(Ar:N_2)1:1, and Ti/TiN-(Ar:N_2)1:3 films. The rates of proliferation of the cells cultured on the Ti/TiN-(Ar:N_2)1:1 and Ti/TiN-(Ar:N_2)1:3 films were much higher than that on the uncoated Co–Cr substrate ($P < 0.05$). This suggests that TiN films can facilitate cell proliferation significantly.

The pre-osteoblasts cells (MC3T3-E1) grown in the presence of serum and ascorbic acid differentiate into osteoblasts and produce an extensive collagenous extracellular matrix that can be mineralized by the addition of β-glycerophosphate [28]. Therefore, the cells were cultured in the medium to induce differentiation. The ALP activity

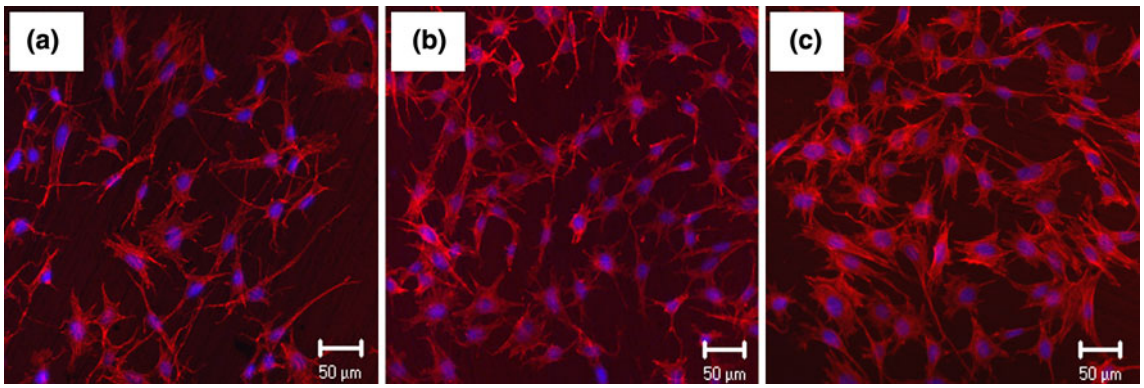

Fig. 6 CLMS of cell attachment on the tested specimens after 24 h of culturing. (**a**) Uncoated Co–Cr, (**b**) Ti/TiN-(Ar:N_2)1:1 film, and (**c**) Ti/TiN-(Ar:N_2)1:3 film

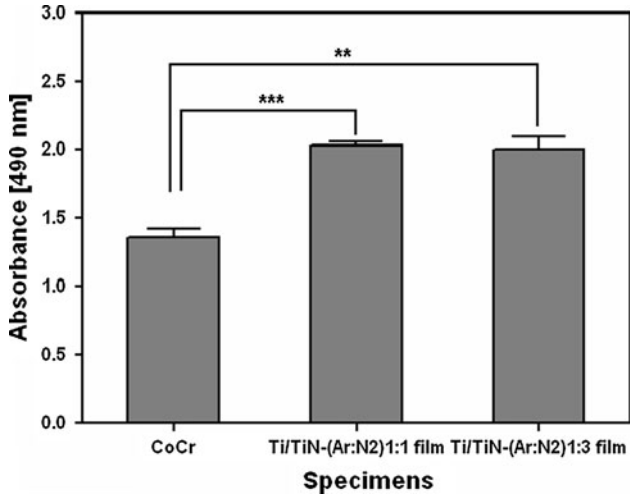

Fig. 7 Proliferation rate of osteoblasts on the specimens after 5 days culture. The *error bar* indicates one standard deviation ($n = 3$). Statistically significant: $^{***}P < 0.001$, $^{**}P < 0.01$

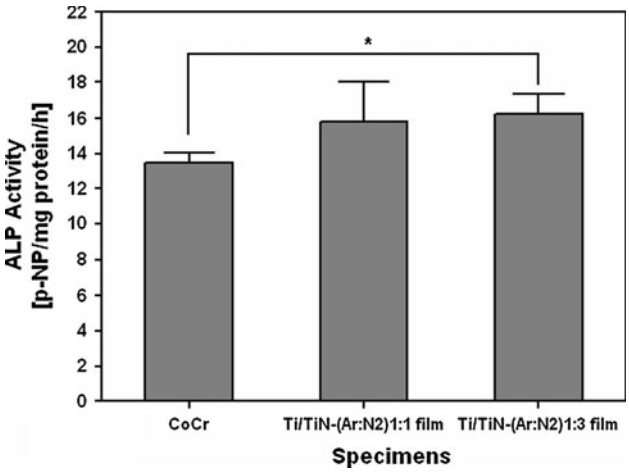

Fig. 8 ALP activity of MC3T3 cells cultured on the specimen for 7 days. The *error bar* indicates one standard deviation ($n = 3$). Statistically significant: $^{*}P < 0.05$

was examined after culturing for 7 days to determine the effect of the TiN films on the cell differentiation. The deposition of TiN films increased the ALP activity significantly, which is a cell surface glycoprotein that is involved in mineralization and is the most widely recognized marker of osteoblastic differentiation [29], as shown in Fig. 8. This suggests that the TiN films facilitated the differentiation of MC3T3-E1 cells. These ALP expression levels, along with the proliferation behavior, provide a good illustration of the improved biocompatibility of the Co–Cr alloy deposited with the TiN films by reactive DC sputtering.

4 Conclusions

Various TiN films (TiN-(Ar/N_2)1:1, Ti/TiN-(Ar/N_2)1:1, and Ti/TiN-(Ar:N_2)1:3) were deposited on Co–Cr substrates using reactive DC sputtering, and their mechanical properties and biocompatibility were evaluated. The use of a Ti interlayer enhanced the adhesion between the Co–Cr substrate and TiN film significantly. The Ti/TiN-(Ar/N_2)1:1 and Ti/TiN-(Ar:N_2)1:3 films showed a dense, columnar microstructure, which led to a considerable increase in mechanical properties, such as critical load, hardness, elastic modulus, and plastic resistance. In addition, deposition of the TiN films improved the biocompatibility of the Co–Cr, which was assessed by an in vitro cell test using a pre-osteoblast cell line.

Acknowledgments This research was supported by WCU (World Class University) project through National Research Foundation of Korea funded by the Ministry of Education, Science and Technology (R31-2008-000-10075-0) and by the Fundamental R&D Program for Core Technology of Materials funded by the Ministry of Knowledge Economy, Republic of Korea.

References

1. Hyslop OJS, Abdelkader AM, Cox A, Fray DJ. Electrochemical synthesis of biomedically implant CoCr alloy. Acta Mater. 2010;58:3124–30.

2. Reclare L, Eschler PY, Lerf R, Blatter A. Electrochemical corrosion and metal ion release from CoCrMo prosthesis with titanium plasma pray coating. Biomaterials. 2005;26:4747–56.
3. Asphahani Aziz I (1988) Corrosion of cobalt-base alloy. In: ASM metal handbook, vol. 13. 9th ed. Kokomo: Haynes International, Inc. 1988. p. 658–68.
4. Goldberg JR, Gilbert JL. The electrochemical and mechanical behavior of passivated and TiN/AlN-coated CoCrMo and Ti6Al4 V alloys. Biomaterials. 2004;25:851–64.
5. Roy ME, Whiteside LA, Xu J, Katerberg BJ. Diamond-like carbon coatings enhance the hardness and resilience of bearing surfaces for use in joint arthroplasty. Acta Biomater. 2010;6:1619–24.
6. Balla VK, Devasconcellos PD, Xue C, Bose S, Bandyopadhyay A. Fabrication of compositionally and structurally graded Ti-TiO_2 structures using laser engineered net shaping (LENS). Acta Biomater. 2009;5:1831–7.
7. Okazaki Y, Gothoh E. Comparison of metal release from various metallic biomaterials in vitro. Biomaterials. 2005;26:11–21.
8. Lin HY, Bumgardner JD. Changes in the surface oxide composition of Co–Cr–Mo implant alloy by macrophage cells and their released reactive chemical species. Biomaterials. 2004;25:1233–8.
9. Arslan E, Iğdil MC, Yazici H, Tamerler C, Bermek H, Trabzon L. Mechanical properties and biocompatibility of plasma-nitrided laser-cut 316 L cardiovascular stents. J Mater Sci: Mater Med. 2008;19:2079–86.
10. Balla VK, Xue W, Bose S, Bandyopadhyay A. Laser-assisted Zr/ZrO2 coating on Ti for load-bearing implants. Acta Biomater. 2009;5:2800–9.
11. Stansky DV, Gloushankova NA, Sheveiko AN, Kharitonova MA, Moizhess TG, Levashov EA, Rossi F. Design, characterization and testing of Ti-based multicomponent coatings for load-bearing medical applications. Biomaterials. 2005;26:2909–24.
12. Chien CC, Liu KT, Duh JG, Chang KW, Chung KH. Effect of nitride film coatings on cell compatibility. Dent Mater. 2008;24:986–93.
13. Han CM, Kim HE, Kim YS, Han SK. Enhanced biocompatibility of Co–Cr implant material by Ti coating and micro-arc oxidation. J Biomed Mater Res B. 2009;90B:165–70.
14. Groessner-schreiber B, Neubert A, Müller WD, Hopp M, Griepentrog M, Lange KP. Fibroblast growth on surface-modified dental implants: an in vitro study. J Biomed Mater Res. 2003;64A:591–9.
15. Pihosh Y, Goto M, Kasahara A, Oishi T, Tosa M. Influence of reacting nitrogen gas consistence on the properties of TiN films prepared by rf. Magnetron sputtering. Appl Surf Sci. 2005;224:244–7.
16. Subramania B, Ashok K, Jayachandran M. Effect of substrate temperature on the structural properties of magnetron sputtered titanium nitride thin films with brush plated nickel interlayer on mild steel. Appl Surf Sci. 2008;255:2133–8.
17. Altun H, Sinici H. Corrosion behavior of magnesium alloys coated with TiN by cathodic arc deposited in NaCl and Na_2SO_4 solutions. Mater Character. 2008;59:266–70.
18. Huang HH, Hsu CH, Pan SJ, He JL, Chen CC, Lee TL. Corrosion and cell adhesion behavior of TiN-coated and ion-nitrided titanium for dental applications. Appl Surf Sci. 2005;244:252–6.
19. Wisbey A, Gregson PJ. Application of PVD TiN coating to Co–Cr–Mo based surgical implants. Biomaterials. 1987;8:477–80.
20. Cyster LA, Grant DM, Parker KG, Parker TL. The effect of surface chemistry and structure of titanium nitride (TiN) films on primary hippocampal cells. Biomol Eng. 2002;19:171–5.
21. Mukherjee S, Maitz MF, Pham MT, Richter E, Prokert F, Moeller W. Development and biocompatibility of hard Ti-based coatings using plasma immersion ion implantation-assisted deposition. Surf Coat Technol. 2005;196:312–6.
22. Pham VH, Yook SW, Li Y, Jeon G, Kim HE, Koh YH. Improving hardness of biomedical Co–Cr by deposition of dense and uniform TiN films using negative substrate bias during reactive sputtering. Mater Lett. 2011;65:1707–9.
23. Pischow KA, Eriksson L, Harju E, Korhonen AS. The influence of titanium interlayers on the adhesion of PVD TiN coatings on oxidized stainless steel substrates. Surf Coat Technol. 1993;58:163–72.
24. Gerth J, Wiklund U. The influence of metallic interlayers on the adhesion of PVD TiN coatings on high-speed steel. Wear. 2008;264:885–92.
25. Carpenter S, Kelly PJ. Sub-microstructure and surface topography of reactive unbalanced magnetron sputtered titanium and titanium compound thin films. Surf Coat Technol. 2009;204:923–6.
26. Cheng Y, Zheng YF. Effect of N_2/Ar gas flow ratio on the deposition of TiN/Ti coatings on NiTi shape memory alloy by PIID. Mater Lett. 2006;60:2243–7.
27. Liu X, Lim JY, Donahue HJ, Dhurjati R, Matro AM, Vogler EA. Influence of substratum surface chemistry/energy and topography on the human fetal osteoblastic cell line hFOB 1.19: phenotypic and genotypic responses observed in vitro. Biomaterials. 2007;28:4535–50.
28. Beck GR Jr, Sullivan EC, Moran E, Zerler B. Relationship between alkaline phosphatase levels, osteopontin expression, and mineralization in differentiating MC3T3-E1 osteoblasts. J Cell Biochem. 1998;68:269–80.
29. Marom R, Shur I, Solomon R, Benayahu D. Characterization of adhesion and differentiation markers of osteogenic marrow stromal cells. J Cell Physiol. 2005;202:41–8.